References and Notes

1. A set of papers on the first results of the Pioneer Venus plasma instruments was published in the 23 February 1979 issue of *Science*. H. A. Taylor, Jr., *et al.*, *Science* **203**, 752 (1979); W. C. Knudsen, K. Spenner, R. C. Whitten, J. R. Spreiter, K. L. Miller, V. Novak, *ibid.*, p. 757; L. H. Brace, R. F. Theis, J. P. Krehbiel, A. F. Nagy, T. M. Donahue, M. B. McElroy, A. Pedersen, *ibid.*, p. 763.
2. L. H. Brace, H. A. Taylor, Jr., P. A. Cloutier, R. E. Daniell, Jr., A. F. Nagy, *Geophys. Res. Lett.* **6**, 345 (1979).
3. L. Colin and D. M. Hunten, *Space Sci. Rev.* **20**, 451 (1977).
4. M. B. McElroy and D. F. Strobel, *J. Geophys. Res.* **74**, 1118 (1969).
5. K. Gringauz, M. J. Verigin, T. K. Breus, T. Gombosi, *ibid.* **84**, 2123 (1979).
6. T. E. Cravens, A. F. Nagy, R. H. Chen, A. I. Stewart, *Geophys. Res. Lett.* **5**, 613 (1978).
7. H. B. Niemann, R. E. Hartle, A. E. Hedin, W. T. Kasprzak, N. W. Spencer, D. M. Hunten, G. R. Carignan, *Science* **205**, 54 (1979).
8. H. G. Mayr, I. Harris, H. S. Porter, *Eos* **59**, 1167 (1978).
9. A. J. Kliore, I. R. Patel, A. F. Nagy, T. E. Cravens, T. I. Gombosi, *Science* **205**, 99 (1979).
10. D. S. Intriligator, H. R. Collard, J. D. Mihalov, R. Whitten, J. H. Wolfe, *ibid.*, p. 116.
11. H. A. Taylor, Jr., H. C. Brinton, S. J. Bauer, R. E. Hartle, P. A. Cloutier, R. E. Daniell, Jr., T. M. Donahue, *ibid.*, p. 96.
12. M. V. Keldysh, *Icarus* **30**, 605 (1977).
13. W. W. L. Taylor, F. L. Scarf, C. T. Russell, L. H. Brace, *Science* **205**, 112 (1979).

14. We are grateful to L. Wharton at Goddard Space Flight Center (GSFC) for aid in modeling the OETP measurements and to T. Cravens and T. Gombosi at the University of Michigan and I. Harris and H. S. Porter at GSFC for computing the electron ionization rates and resulting electron density profiles.

21 May 1979

Thermal Structure and Energy Influx to the Day- and Nightside Venus Ionosphere

Abstract. *Pioneer Venus in situ measurements made with the retarding potential analyzer reveal strong variations in the nightside ionospheric plasma density from location to location in some orbits and from orbit to orbit. The ionopause is evident at night as a relatively abrupt decrease in the thermal plasma concentration from a few hundred to ten or fewer ions per cubic centimeter. The nightside ion and electron temperatures above an altitude of 250 kilometers, within the ionosphere and away from the terminator, are comparable in magnitude and have a value at the ionopause of approximately 8000 K. The electron temperature increases from a few tens of thousands of degrees Kelvin just outside the ionopause to several hundreds of thousands of degrees Kelvin further into the shocked solar wind. The coldest ion temperatures measured at an altitude of about 145 kilometers are 140 to 150 K and are still evidently above the neutral temperature. Preliminary day- and nightside model ion and electron temperature height profiles are compared with measured profiles. To raise the model ion temperature to the measured ion temperature on both day- and nightsides, it was necessary to include an ion energy source of the order of* 4×10^{-3} *erg per square centimeter per second, presumably Joule heating. The heat flux through the electron gas from the solar wind into the neutral atmosphere averaged over day and night may be as large as 0.05 erg per square centimeter per second. Integrated over the planet surface, this heat flux represents one-tenth of the solar wind energy expended in drag on the sunward ionopause hemisphere.*

In our earlier report we presented ion and electron temperatures and major ion composition data for six of the first ten orbits selected as representative of the dayside Venus ionosphere at a solar zenith angle (SZA) of about 70° (*1*). The ionosphere below the ionopause at that location appeared to be relatively constant in total ion concentration, ion and electron temperature, and ion composition. Strong changes did occur when the solar wind depressed the ionopause height to 300 km on orbit 9, but nonetheless a fairly consistent picture of the ionosphere appeared to have been achieved.

In contrast, the ionosphere on the nightside shows strong variations from location to location within some single orbits and from one orbit to the next (Fig. 1). The in situ measurements made by the Pioneer Venus retarding potential analyzer (RPA) experiment and companion experiments (*2*) are substantiating the existence of strong nightside ionospheric variability initially inferred from earlier radio occultation experiments (*3*) and are revealing its nature in more detail. Orbit 51 is representative of those orbits for which the nightside ion concentration is at its maximum value. Orbit 92 is representative of a minimum nightside ionosphere. Orbit 65 is intermediate. The ionopause is usually evident as a rather abrupt decrease in concentration from a few hundred to ten or fewer ions per cubic centimeter. Frequently, the ion concentration increases to a few hundred per cubic centimeter for a period of time before the final decrease in concentration. This behavior suggests an irregular ionopause surface or patches of detached ionospheric plasma. The concentrations in Fig. 1 are plotted as a function of altitude but are not "vertical" profiles inasmuch as the spacecraft is also moving horizontally. The total concentrations are derived from the ion saturation currents and are not corrected for ion drift velocity.

Strong variations in plasma concentration within a single orbit are illustrated in the lower half of Fig. 2. The wavelike variations are most pronounced at low altitude and decrease with altitude. The spacecraft travels approximately 1500 km horizontally between the major peaks in plasma density. At the higher altitudes, the plasma diffusion coefficient becomes large and diffusion is evidently able to smooth out the strong variations observed at low altitude. The relative plasma density is measured from the saturation current of the electron mode and is not as precise a measurement of the plasma density as that obtained in the ion mode (*1*).

The strong variation in the nightside ion concentration with time and location requires a strong variation in the ionization source mechanism, loss mechanism, or plasma transport mechanism. A determination of which of these mechanisms

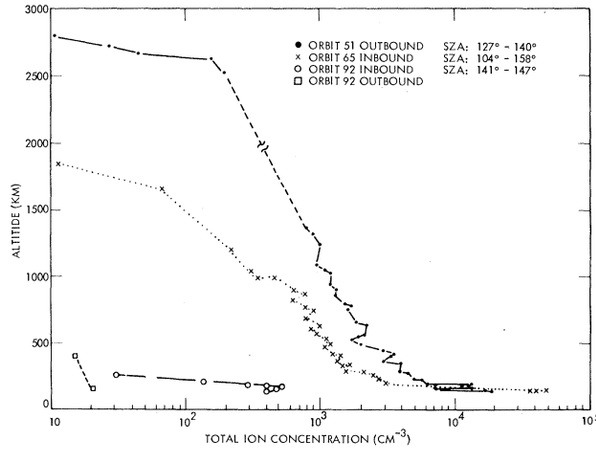

Fig. 1. Total ion concentrations for three representative nightside orbits, illustrating large orbit-to-orbit variation.

0036-8075/79/0706-0105$00.50/0

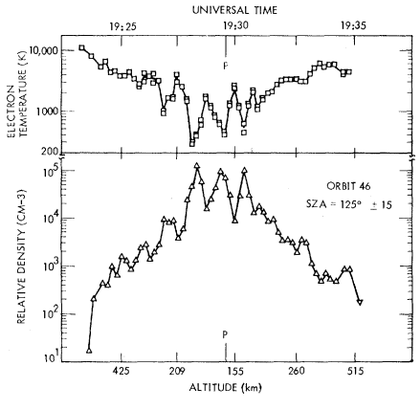

Fig. 2. Electron density and corresponding electron temperature for nightside orbit 46, P = periapsis. Large wavelike variations in electron density at low altitude within one orbit are illustrated. The electron temperature responds to variations in electron density in the expected manner.

is the most significant will be the subject of future investigations.

Nightside ion temperature profiles derived from a few selected orbits are presented in Fig. 3. The orbits selected were those with higher plasma concentration. Ion temperatures at high altitude on the inbound legs differed systematically from those of the outbound leg and will not be discussed in this report. The outbound leg is more representative of a vertical profile at large SZA. Contrary to our expectations, the ion temperature above an altitude of approximately 225 km is larger by a factor of 2 or more than

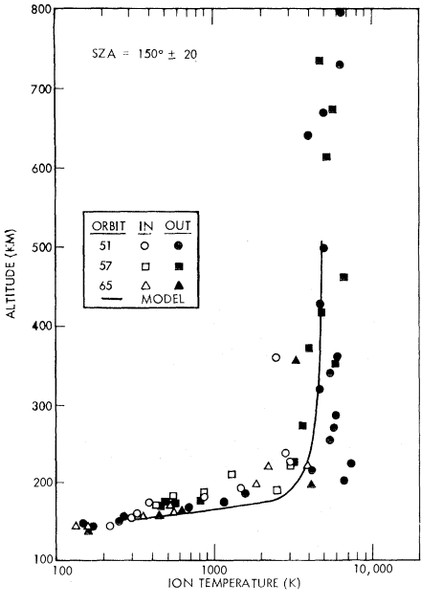

Fig. 3. Nightside ion temperatures from three selected orbits. Ion temperatures are comparable to the electron temperatures (Fig. 4). The model ion temperature curve was derived for a column heat input of 5×10^{-3} erg cm^{-2} sec^{-1} uniformly distributed between altitudes of 150 and 500 km.

it is on the dayside (*1*). Above this altitude on the outbound leg the ion and electron temperatures (Fig. 4) are comparable. The coldest ion temperatures measured at periapsis are 140 to 150 K and are comparable to but higher, evidently, than the neutral temperature (*4*). The ion temperature should not show such a strong vertical temperature gradient if the ions were equilibrated with the neutrals at the lowest altitudes. The model temperature illustrated represents a preliminary attempt to reproduce the observed ion temperature. The model was arbitrarily given an ion concentration and composition measured by the RPA and a heat input of 5×10^{-3} erg cm^{-2} sec^{-1} uniformly distributed between 150 and 500 km. Heating of the thermal electrons by photoelectrons (on the dayside) and thermal exchange between ion and electron gases are included as well as energy loss to the neutral gas.

The electron temperature T_e on the nightside is comparable to that on the dayside. Figure 4 shows measured temperatures for several orbits from altitudes of 150 to 800 km. The model curve illustrated is the expected T_e variation in a spherically symmetric electron gas through which heat is being conducted and which has a temperature of 300 K at a radius of 6200 km (altitude, 148 km). If the effect of the magnetic field on the thermal conductivity may be neglected or if the field is substantially radial in direction, the heat flux is approximately 0.07 erg cm^{-2} sec^{-1}. The T_e increases abruptly from approximately 8000 K inside the ionophere to a few tens of thousands of degrees Kelvin just outside the ionopause. Further into the shocked solar wind, the temperature increases to a few hundreds of thousands of degrees Kelvin.

Quite generally, T_e varies oppositely to the electron concentration. Transfer of heat from the electron gas to both the neutral and ion gases increases with an increase in electron concentration (*5*). The large variations in T_e observed below 250 km on orbit 46 are evidently in response to the large concentration variations (Fig. 2).

We have reanalyzed ion temperatures from a few dayside orbits, using information on the minor ion concentrations provided by the orbiter instruments (*6*). These revised temperatures, together with the T_e measured on the same orbits, are presented in Fig. 5. The ion temperatures between altitudes of 150 and 250 km were lowered by this reanalysis approximately 100 K below the values presented earlier. The solid lines are model

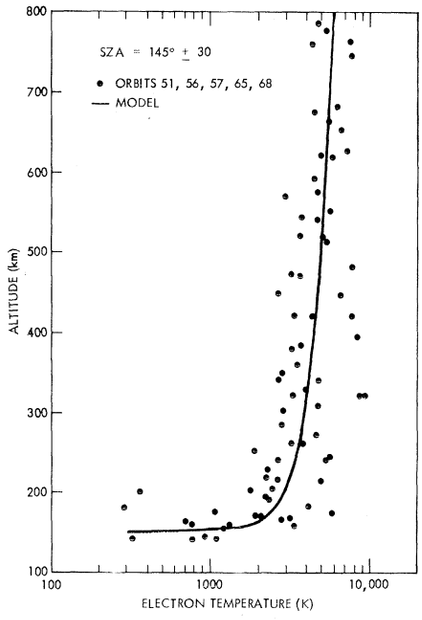

Fig. 4. Nightside electron temperature data from both inbound and outbound legs of several orbits. The large scatter at low altitude is real (see Fig. 2). The model electron temperature curve was derived on the assumption that heat was being conducted from above. For a near-vertical magnetic field, the heat flux is 0.07 erg cm^{-2} sec^{-1}.

temperatures. The model included a heat input to the electrons at the 500-km boundary of 3×10^{-2} erg cm^{-2} sec^{-1}. Between 150 and 250 km, a uniformly distributed energy input to the ion gas of 3×10^{-3} erg cm^{-2} sec^{-1} was included to raise the ion temperature above the neutral gas temperature. This energy input is presumably from Joule heating. Heating of the ions by dissociative charge ex-

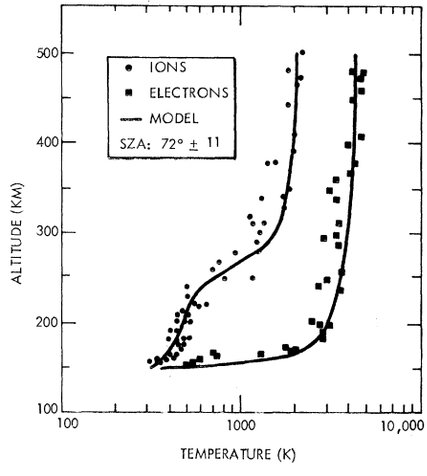

Fig. 5. Dayside ion and electron temperature profiles. A column heat input of 3×10^{-3} erg cm^{-2} sec^{-1} uniformly distributed between altitudes of 150 and 250 km and presumably representing Joule heating was required to raise the model ion temperature to the measured temperature in this altitude interval. The model included an electron heat input at the top of 3×10^{-2} erg cm^{-2} sec^{-1} (see text).

change production of energetic O_2^+ (7) is estimated to be less by an order of magnitude than that needed to raise the ion temperatures to the measured temperature. A small heat input to the ions of 1.7×10^{-4} erg cm^{-2} sec^{-1} uniformly distributed in altitude above 230 km was included to bring the model ion temperatures at high altitude into agreement with the measurements. Solar wind heating or Joule heating, or both, are possible sources for this heating. This latter ion heat input is approximately half of that which Cravens *et al.* had assumed would be present prior to the Pioneer Venus measurements (8).

We have assumed in the above computations of heat flux through the electron gas for both day and night that the magnetic field is sufficiently weak to be neglected or, equivalently, that the field is parallel to the heat flow. However, a magnetic field with a magnitude of 1 gamma and perpendicular to the direction of heat flow is expected to greatly reduce the heat conductivity. We have found it possible to match the observed dayside electron temperature profile reasonably well by reducing the heat conductivity by 20 percent and assuming no heat influx at the top boundary. With this modification, photoelectron heating of the electron gas was sufficient to heat the electrons to the observed temperature. Nevertheless, the electron gas heat conductivity within the ionosphere must be substantially greater than it is in the region of the ionopause boundary. The rapid decrease in T_e is going from the shocked solar wind into the ionosphere and the nearly constant temperature with altitude just inside the ionosphere imply an increase in the thermal conductivity within the ionosphere.

If the electron gas within the ionosphere has a conductivity that is close to its magnetic field-free value ($K_{ei} = 9 \times 10^{-7}\ T_e^{(5/2)}$ erg cm^{-1} sec^{-1} K^{-1}), it will conduct into the neutral atmosphere a substantial fraction of the solar wind energy expended in drag on the sunward ionopause hemisphere. The heat flux Q through the electron gas averaged over the day- and nightsides will be of the order of 0.05 erg cm^{-2} sec^{-1}. The energy expended in drag is equal to the product of the solar wind velocity v and the pressure $nm_pv^2 \cos^2$ SZA integrated over the sunward ionopause hemisphere, where n is the solar wind proton concentration and m_p is the proton mass. Thus, the upper bound for the fraction f of heat conducted into the atmosphere becomes

$$f = \frac{4\pi r^2 \cdot Q}{\pi r^2 \cdot 1/2 n m_p v^3} \simeq 0.1$$

where r is the radius of the ionopause. We have taken n to be 20 cm^{-3} and v to be 450 km sec^{-1}. This is a significant fraction of the expended energy and has significant implications for the theory of the solar wind–ionosphere interaction.

W. C. KNUDSEN
Lockheed Palo Alto Research Laboratory, Palo Alto, California 94304
K. SPENNER
Institut für Physikalische Weltraumforschung der Fraunhofer Gesellschaft, 78 Freiburg, West Germany
R. C. WHITTEN
NASA Ames Research Center, Moffett Field, California 94035
J. R. SPREITER
Stanford University, Stanford, California 94305
K. L. MILLER
Lockheed Palo Alto Research Laboratory
V. NOVAK
Institut für Physikalische Weltraumforschung der Fraunhofer Gesellschaft

References and Notes

1. W. C. Knudsen, K. Spenner, R. C. Whitten, J. R. Spreiter, K. L. Miller, V. Novak, *Science* **203**, 757 (1979).
2. L. H. Brace, H. A. Taylor, Jr., P. A. Cloutier, R. E. Daniell, Jr., A. F. Nagy, *Geophys. Res. Lett.*, in press; H. A. Taylor, Jr., H. C. Brinton, S. J. Bauer, R. E. Hartle, P. A. Cloutier, R. Daniell, F. C. Michel, T. M. Donahue, *Science* **205**, 96 (1979); L. H. Brace, R. F. Theis, H. B. Niemann, H. G. Mayr, W. R. Hoegg, A. F. Nagy, *ibid.*, p. 102.
3. H. T. Howard, G. L. Tyler, G. Fjeldbo, A. J. Kliore, G. S. Levy, D. L. Brunn, R. Dickinson, R. E. Edelson, W. L. Martin, R. B. Postal, B. Seidel, T. T. Sesplaukis, D. L. Shirley, C. T. Stelzried, D. N. Sweetnam, A. I. Zygielbaum, P. B. Esposito, J. D. Anderson, I. I. Shapiro, R. D. Reasenberg, *Science* **183**, 1297 (1974); Iu. N. Aleksandrov, M. B. Vasiliev, A. S. Vyshlov, G. G. Dolbezhev, A. L. Zaitzev, M. A. Kolosov, G. M. Petrov, N. A. Savich, V. A. Samovol, *Kosm. Issled.* **14**, 824 (1976).
4. H. B. Niemann, R. E. Hartle, A. E. Hedin, W. T. Kasprzak, N. W. Spencer, D. M. Hunten, G. R. Carignan, *Science* **205**, 54 (1979).
5. P. M. Banks and G. Kockarts, *Aeronomy* (Academic Press, New York, 1973), part B.
6. H. A. Taylor, Jr., *et al. Science* **203**, 752 (1979).
7. R. P. Rohrbaugh, J. S. Nisbet, E. Bleuler, J. R. Herman, *J. Geophys. Res.*, in press.
8. T. E. Cravens, A. F. Nagy, R. H. Chen, A. I. Steward, *Geophys. Res. Lett.* **5**, 613 (1978).
9. The retarding potential analyzer experiment is supported by NASA through contract NAS2-9481 and by the Bundesminister für Forschung and Technologie through contract 01 Do 238 (RV 14-B 28/73).

15 May 1979

Comparison of Calculated and Measured Ion Densities on the Dayside of Venus

Abstract. *Data from the Pioneer Venus ion mass spectrometers are compared with model calculations of the ion density distributions appropriate for daytime conditions. The model assumes diffusive equilibrium upper boundary conditions for the major ions (O_2^+, O^+, CO_2^+, He^+, and H^+); the agreement between the calculated and measured gross behavior of these ions is reasonably good except for H^+, which may be influenced strongly by convective transport processes. The distributions of five minor ions (C^+, N^+, NO^+, CO^+, and N_2^+) are also calculated for the chemically controlled region ($\lesssim$ 200 kilometers); the agreements are, in general, poor, an indication that our present understanding of the Venus minor ion chemistry is still incomplete.*

Data from the Pioneer Venus instrument complement (*1*) are providing the most comprehensive set of observations ever obtained of a planetary ionosphere-atmosphere system other than the terrestrial one. The purpose of this report is to present the results of model calculations of the ion density distribution of the dayside Venus ionosphere and to compare these with the observed

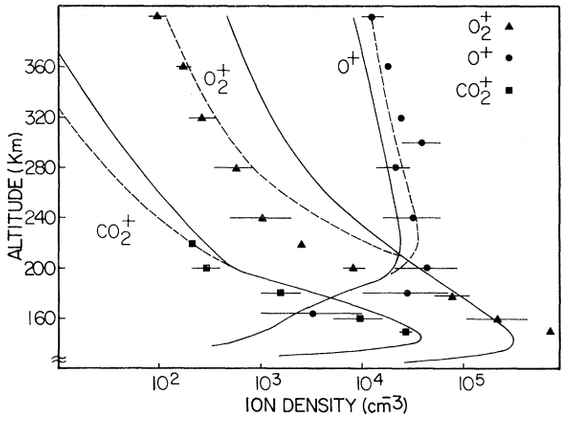

Fig. 1. Calculated ion density profiles for O^+, O_2^+, and CO_2^+. Data from OIMS and BIMS are also shown. The curves with dashed lines are for inhibited diffusion coefficients.

0036-8075/79/0706-0107$00.50/0